DOI: 10.1002/ejic.201100104

Structure and Composition of the Layered Double Hydroxides of Mg and Fe: Implications for Anion-Exchange Reactions

G. V. Manohara,[a] S. V. Prasanna,[a] and P. Vishnu Kamath*[a]

Keywords: Ion exchange / UV/Vis spectroscopy / Magnesium / Iron / Hydroxides

Partial cation exchange of Mg^{2+} ions with Fe^{3+} ions employing solid $Mg(OH)_2$ as precursor yielded an ordered layered double hydroxide of Mg and Fe in the presence of carbonate anions. Structure refinement revealed that the compound adopts the polytype structure $3R_1$ (space group $R\bar{3}m$, a = 3.108 Å, c = 23.08 Å) and does not show any signs of cation order. It crystallizes with a unique cation ratio of [Mg]/[Fe] = 4. At this ratio, the compound shows a single sharp absorption in its electronic spectrum at 280 nm. Attempts to prepare the LDH with a higher Fe content resulted in the phase separation of excess Fe into X-ray amorphous binary compounds, the existence of which can be discerned only by the appearance of absorptions at $\lambda > 350$ nm, a characteristic of oxide–hydroxides of Fe^{3+}. The nitrate-containing compound also forms with a similarly low Fe content. At this composition, the compound does not exhibit any anion-exchange properties as the nitrate ions intercalated in layered hydroxides of low layer charge are not labile. This explains the paucity of information on anion-exchange reactions of layered double hydroxides of Mg and Fe.

Introduction

The layered double hydroxide (LDH) of Mg and Fe has potential applications in catalysis,[1] water purification,[2,3] safe storage of vitamins,[4] anion exchange,[5] as well as cation sorption.[6] The oxide residue obtained by the thermal decomposition of the Mg/Fe LDH is a bifunctional catalyst with both acidic and basic surface sites.[7] The $Fe^0/Fe^{2+}/Fe^{3+}$ composition of the catalyst can be finely tuned by controlled reduction, whereby catalysts with high olefin selectivity can be generated for use in the Fischer–Tropsch reaction. Given the magnetic properties of the oxides of Fe^{III}, the Mg/Fe LDH is also used as a precursor for the synthesis of single-phase magnetic ferrites[8] and magnetic nanocomposites.[9] Furthermore, the Mg/Fe LDH is less toxic than many combinations of di- and trivalent cations and is proposed as a model medium for drug delivery.[10]

The Mg/Fe LDH is obtained by the isomorphous substitution of a fraction x of Mg^{2+} ions by Fe^{3+} ions in $Mg(OH)_2$ to yield positively charged layers with the composition $[Mg_{1-x}Fe_x(OH)_2]^{x+}$.[11] Anions are incorporated into the interlayer. Many pairs of di- and trivalent cations can be combined with a variety of anions[12–14] to obtain a large and diverse family of layered double hydroxides. The Mg/Fe LDH in many ways stands apart from other LDHs.

(1) There is limited literature on the anion-exchange and -uptake properties of the pristine and calcined Mg/Fe LDH. Evidence for the anion-exchange of Mg/Fe LDHs is at best equivocal and there are some definitive reports,[4] including this work, of the absence of anion-exchange reactions in Fe-containing LDHs.

(2) In general, the a parameter of LDHs decreases with increasing trivalent metal content.[15] In the case of Mg/Fe LDHs, there are reports that the a parameter remains invariant with Fe^{3+} content,[16] thereby raising the question: Is the composition of the Mg/Fe LDH fixed? If so, at what value of x?

(3) If the composition is fixed at x = 0.25, as suggested by some authors,[17] or at x = 0.2, as suggested by others,[5,18] does the Mg/Fe LDH crystallize in a cation-ordered structure?[17]

The answers to these questions have not been forthcoming on account of the absence of precise structural information on Mg/Fe LDHs. There are few, if any, ordered preparations of Mg/Fe LDHs that could facilitate structure refinement. The Mg/Fe LDH has been prepared by addition of a mixed metal (Mg^{2+} + Fe^{3+}) salt solution to a solution of NaOH,[17] Na_2CO_3,[19] or $NaHCO_3$[20] at a high constant pH. The solubility product of "$Fe(OH)_3$" at 10^{-33} is far below that of $Mg(OH)_2$ at 10^{-10}.[21] Thereby, coprecipitation reactions do not yield single-phase products, but generate copious amount of X-ray amorphous unitary products of Fe^{3+}. The LDH is also obtained under these conditions, but is highly disordered as a result of short nucleation times. Homogeneous precipitation from solution (HPFS) by hydrolysis of urea[22] or hexamethylenetetramine[23] is successful in generating ordered LDHs as it reduces the rate of crystal growth around the nuclei. However, HPFS is unsuccessful in the Mg/Fe system as the "$Fe(OH)_3$" gel precipitates in preference to other phases.[24]

[a] Department of Chemistry, Central College, Bangalore University,
Bangalore 560 001, India

Supporting information for this article is available on the WWW under http://dx.doi.org/10.1002/ejic.201100104.

Another approach is to coprecipitate Mg^{2+} and Fe^{2+} ions into a single phase brucite-like hydroxide precursor in a reducing atmosphere.[8b,8c] This precursor is then oxidized in the ambient in the presence of dissolved sulfates to obtain the LDH. This synthesis envisages an oxidative intercalation of anions. Although the synthesis was successful, it did not yield an ordered phase.

In this paper, we report the synthesis of an ordered Mg/Fe–CO_3 LDH by cation exchange by the reaction of solid $Mg(OH)_2$ with dissolved Fe^{3+} ions. Structure refinement reveals that the LDH adopts a cation-disordered structure belonging to the $R\bar{3}m$ space group.

Results and Discussion

Brucite consists of stacks of charge-neutral metal hydroxide layers with the composition $[Mg(OH)_2]$.[25] The layers are held together by van der Waal's forces and the interlayer region does not contain any intercalated moieties, giving a basal spacing of only 4.7 Å. A reflection is seen at this value (2θ = 18.8°) in the PXRD pattern. $Mg(OH)_2$ exhibits no interlayer chemistry. The Mg/Fe LDH, on the other hand, includes intercalated anionic species together with water molecules in the interlayer gallery. The basal spacing is dependent on the size of the intercalated anion. Intercalated carbonate yields a basal spacing of 7.6 Å (2θ = 11.6°), which corresponds to the 003 reflection. The higher harmonic, 006, is seen at 3.8 Å (2θ = 23.4°). The transformation of $Mg(OH)_2$ to the LDH can be monitored by these characteristic reflections.

Figure 1 shows the powder XRD patterns of the solid obtained by soaking $Mg(OH)_2$ in a solution of Fe^{3+} for different times. At short ageing times, unreacted $Mg(OH)_2$ is seen to coexist with the LDH phase. It is interesting to observe that the solid obtained after soaking and immediate separation (soaking time ca. 1–5 min) shows the presence of the LDH. With an increase in soaking time, the reflections due to the LDH grow in intensity, whereas the 4.7 Å reflection due to $Mg(OH)_2$ progressively decreases in intensity. After 120 h, the reflections due to $Mg(OH)_2$ are completely extinguished and a single-phase LDH is obtained.

The growth of the LDH can also be seen by monitoring the 110 reflection of the LDH. With an increase in ageing time, this reflection is found to shift to higher 2θ values, from 58.8 to 59.6° (see inset in Figure 1). The a parameter of the LDH, estimated to be $a = 2d_{110}$, is found to decrease from 3.14 to 3.10 Å on ageing. Because Mg^{2+} has a higher (0.86 Å) octahedral ionic radius than Fe^{3+} (0.785 Å),[26] the decreasing a parameter indicates progressive incorporation of Fe^{3+} ions from solution into solid $Mg(OH)_2$. This behavior is evidence of cation exchange, that is, exchange of Mg^{2+} from the solid for Fe^{3+} from solution, along with the simultaneous insertion of CO_3^{2-} ions from solution into the interlayer. If the LDH was to form by dissolution/reprecipitation, a Fe^{3+}-rich LDH would be expected to form at short ageing times followed by a progressive decrease in the Fe^{3+} content. This would lead to a progressive increase in the a parameter with ageing time.

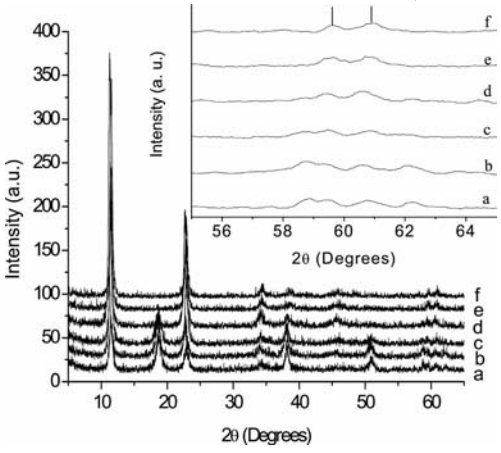

Figure 1. PXRD pattern of Mg/Fe–CO_3 LDHs obtained after different durations of cation exchange: (a) 5 min, (b) 24, (c) 48, (d) 72, (e) 96, and (f) 120 h. The inset shows the high-angle region in detail. Vertical bars in the inset correspond to the 110 and 113 reflections of the LDH.

Cation-exchange reactions are well known in cationic clays. Exchange reactions mainly involve intercalated species. In this sense, from a structural point of view, cation exchange is not expected in layered hydroxides. From the point of view of thermodynamics, Navrotsky and coworkers[27] have shown that the enthalpy of formation of LDHs fits the "mechanical mixture" model because the enthalpy of the LDH is simply a sum of the enthalpies of the divalent metal hydroxide, trivalent metal hydroxide, and the metal carbonate. As "$Fe(OH)_3$" has a much lower solubility product (10^{-33}) than $Mg(OH)_2$ (10^{-10}), it is also thermodynamically more stable than $Mg(OH)_2$. Therefore the exchange of Mg^{2+} for Fe^{3+} is thermodynamically favored. Given the thermodynamic feasibility, the question arises: What are the possible pathways by which such an exchange can take place? In this we are greatly aided by the suggestions made in the literature[28,29] that cation exchange in LDHs takes place by "diadochy" in which the outgoing metal ion exits through the triangular face of the $[M(OH)_6]$ octahedron which lines the interlayer region. The incoming cation likewise enters the coordination sphere by the same pathway. In this case, to synthesize a LDH, the Mg^{2+} ion in brucite is exchanged for the trivalent metal ion in solution.

A series of samples were prepared by varying the relative amounts of Mg^{2+} and Fe^{3+} used for the synthesis (Figure 2). As ageing is carried out in a carbonate-rich medium, there is buffering action and the pH remains in the range of 9.98 ± 0.03 for the entire ageing time of 120 h. At this high pH, most cations are precipitated as hydroxides. Nevertheless, the a parameter remains invariant within the limits of experimental error ($\cong \pm 0.05° 2\theta$) for compositions $x \geq 0.2$ (Table 1). This suggests that $x = 0.2$ ($[M^{2+}]/[M^{3+}] = 4$) is the limiting composition, in keeping with earlier observations,[18] and when the nominal composition x exceeds 0.2, the additional Fe^{3+} is not incorporated into the LDH crystal but phase separates into X-ray amorphous unitary phases. Chemical analysis (Table 1) also reveals that the

Table 1. Unit cell parameters and chemical analysis data for the LDHs. Values in parantheses are expected from the molecular formulae.

[Mg]/[Fe]		Mass [%]		Water content [%]	Cell parameters		Approximate formula
Nominal	Observed	$[Mg^{2+}]$	$[Fe^{3+}]$		*a* [Å]	*c* [Å]	
2	2.4	21.0 (18.5)	20.0 (21.1)	11.3 (11)	3.10	22.96	$Mg_{0.71}Fe_{0.29}(OH)_2(CO_3)_{0.145}\cdot 0.6H_2O$ (S1)
3	2.2	21.0 (21.5)	22.2 (16.5)	12.5 (11.8)	3.10	23.17	$Mg_{0.69}Fe_{0.31}(OH)_2(CO_3)_{0.155}\cdot 0.5H_2O$ (S2)
4	3.5	23.0 (23.4)	15.4 (13.4)	12.3 (14.3)	3.11	23.45	$Mg_{0.78}Fe_{0.22}(OH)_2(CO_3)_{0.11}\cdot 0.7H_2O$ (S3)

best match between the nominal and observed compositions is seen for the sample with nominal $x = 0.2$. This is unlike other LDHs, such as those of Zn/Ga[30] and Zn/Cr,[31] which crystallize with a fixed composition, $x = 0.33$ ($[M^{2+}]/[M^{3+}] = 2$), and the LDH of Mg/Al, which shows a continuous variation in composition, $0.2 \leq x \leq 0.33$ ($2 \leq [M^{2+}]/[Al^{3+}] \leq 4$).[12]

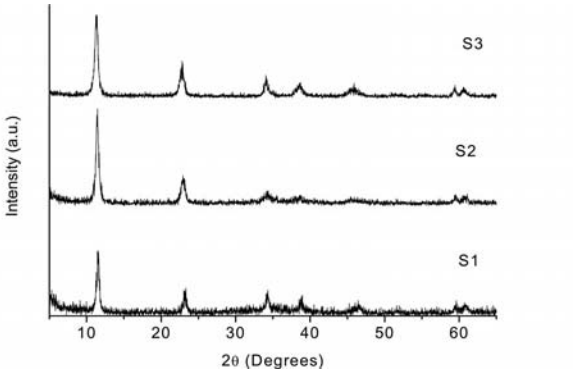

Figure 2. PXRD patterns of Mg/Fe–CO_3 LDHs with different nominal [Mg]/[Fe] ratios.

The crystallinity of all the samples greatly improved on hydrothermal treatment and one representative sample (composition $x = 0.2$, $[M^{2+}]/[M^{3+}] = 4$) was employed for structure refinement by the Rietveld method. The observed pattern was first indexed (see Table S1 for the list of *d* spacings; figure of merit = 13) and the reflection conditions (00*l*, $l = 3n$ and *hkl*, $-h + k + l = 3n$) reveal the crystal symmetry to be rhombohedral. In contrast, mineral forms of the Mg/Fe LDH are reported to crystallize in both rhombohedral and hexagonal crystal systems in the space groups $R\bar{3}$, $R3m$, $R\bar{3}m$, $P6_3/mmc$, and $P6_3/mcm$. One instance of mineral pyroaurite (space group $R\bar{3}m$, CSD-80876) incorporates cation order. Other mineral samples with cation disorder also belong to the same space group. Because no structure models for synthetic Mg/Fe–CO_3 LDHs are available, all mineral structure models of rhombohedral symmetry were considered. A POWDERCELL[32] simulation of the XRD patterns of all the model mineral structures was first carried out and compared with the observed pattern. None of these simulations, except that of the cation-disordered structure in the $R\bar{3}m$ space group, matched with the experimental pattern. In this manner, the possibility of cation ordering was ruled out.

Despite crystal growth on hydrothermal treatment, some anisotropy in the peak shapes could be seen. For instance, the peak due to the 018 reflection is broader (FWHM = 1.0°) than that due to the 012 reflection (FWHM = 0.4°). A satisfactory Rietveld fit (Figure 3) could be obtained only after the inclusion of the anisotropy parameter and the refinement of the components of the corresponding strain tensors. The refined values of the structural and nonstructural parameters together with the goodness-of-fit parameters are given in Tables 2–4.

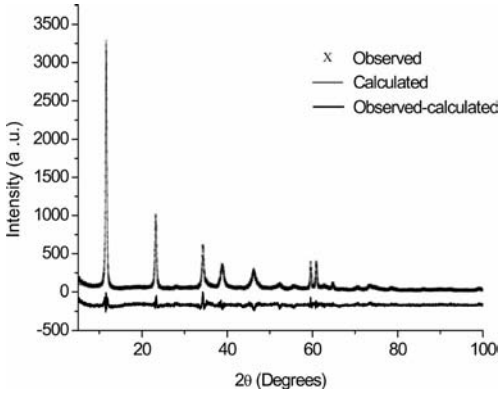

Figure 3. A Rietveld fit of the PXRD pattern of the Mg/Fe–CO_3 LDH ($x = 0.2$).

Table 2. Crystal data and structure refinement parameters of the Mg/Fe–CO_3 LDH.

Crystal system	trigonal
Space group	$R\bar{3}m$
a [Å]	3.1078(18)
c [Å]	23.0798(18)
Volume [Å^3]	193.05(23)
Data points	4750
Parameters refined	49
R_{wp}	0.1751
R_p	0.1319
R (F^2)	0.1166
χ^2	2.6
R_{exp}	0.1079

Table 3. Atomic position parameters of the Mg/Fe–CO_3 LDH obtained from refinement.

Atom type	Wyckoff position	*x*	*y*	*z*	SOF	U_{iso} [Å]
Mg	3a	0	0	0	0.8	0.0251
Fe	3a	0	0	0	0.2	0.0200
O1	6c	0	0	0.3763(2)	1.00	0.0230
O2	18h	0.1280(4)	0.8719(9)	0.4955(4)	0.166	0.0045
C	6c	0.3333	0.6667	0.5061(5)	0.05	0.0473
H1	6c	0	0	0.4445 (5)	1.00	0.0260
H2	6c	0.3333	0.6667	0.5125(5)	0.50	0.0250

The metal–O1 (O1 is the O atom of the hydroxy group) distance of 2.05 Å and O1–O1 distances of 2.677 and 3.108 Å match with the reported values for the mineral $Mg_6Fe_2(OH)_{16}CO_3\cdot 4H_2O$ (pyroaurite).[33] The short O1–O1

Table 4. Bond lengths and angles of the Mg/Fe–CO_3 LDH obtained from Rietveld refinement.

Atom distances [Å]	
(Mg,Fe)–O1	2.0510 (10)
(O1–O1) shared	2.6773 (14)
(O1–O1) in-plane	3.1078 (18)
C–O2	1.1317 (6)
O1–O2	3.7392(19)
M–O2	4.0578 (27)
Bond angles [°]	
O1–(Mg,Fe)–O1	98.51 (3)
O1–(Mg,Fe)–O1	81.48 (3)
O2–C–O2	119.94(0)

distance corresponds to the nonbonding distance measured along the edge shared by two metal–hydroxy coordination polyhedra parallel to the stacking direction. The long O1–O1 contact corresponds to the in-plane edge perpendicular to the stacking direction. The O1–M–O1 angles deviate from 90° so that the metal coordination symmetry is reduced to D_{3d}.

The anisotropic broadening of the profile function modeled in the Rietveld procedure has a phenomenological basis. The refined structure corresponds to the $3R_1$ rhombohedral polytype[34] with the metal hydroxide layers stacking in the sequence AC CB BA AC…. This polytype has prismatic interlayer sites. Another closely related structure with prismatic sites is that of the $2H_1$ polytype with the stacking sequence AC CA AC…. Enthalpically, these two polytypes are very similar[35] and thereby intergrowth of the two polytypes cannot be avoided. The powder XRD patterns of the intergrowth can be conveniently simulated by using the Fortran code DIFFaX.[36] For the purpose of the simulation, the cell parameters and atomic coordinates of the Mg/Fe–CO_3 LDH were taken from the results of the structure refinement. The experimental profile matches that simulated (Figure 4) for an intergrowth of 20% $2H_1$ stacking motifs in a matrix of the $3R_1$ polytype. The crystal strain responsible for the observed anisotropy in the peak shapes essentially originates from the intergrowth of $2H_1$ and $3R_1$ motifs within the same crystal. The first coordination shell of the cations and anions are very similar in the two polytypes. Crystal strain arises due to differences in the outer coordination shells. The main difference is in the arrangement of the cations. In the $3R_1$ polytype, the cations are staggered as b a c b a c…, in the $2H_1$ polytype, the cation positions are eclipsed as b b b b. In a crystal containing random intergrowth of the two polytypes, these differences result in crystal strain.

There is much discussion in the literature on the color of Mg/Fe LDHs. Whereas LDHs with $x \leq 0.25$ are reported to have a light-rose color, those with $x > 0.25$ ($[M^{2+}]/[M^{3+}] \approx 2$) are reported to have a dirty-brown color.[16] The visible absorption spectrum of the Mg/Fe LDH is associated with the coordination symmetry of the Fe^{3+} ion. Within the LDH structure all cations occupy the six-coordinate site of D_{3d} symmetry. This symmetry is a result of the departure

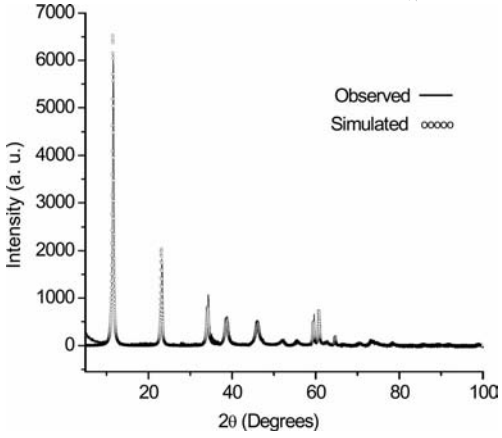

Figure 4. DIFFaX-simulated PXRD pattern of the Mg/Fe–CO_3 LDH overlaid on the experimental pattern. The simulated pattern corresponds to the structure of the $3R_1$ polytype containing planar stacking faults with the local structure of the $2H_1$ polytype.

of the O1–M–O1 angle from 90°. The energy of the crystal field splitting in this symmetry is not very different to that of octahedral symmetry. Fe^{3+} has a low octahedral crystal field stabilization energy (CFSE) within the hydroxide sublattice. Therefore no hydroxide of Fe^{3+} analogous to $Al(OH)_3$ exists. The "$Fe(OH)_3$" is generally a gel with the general composition $Fe_2O_3{\cdot}nH_2O$. The well-defined hydroxide of Fe^{3+} has the formula FeO(OH), which exists in many polymorphic modifications.[37] The phase that forms under conditions close to the synthesis of LDHs is the α-FeO(OH), which is a dirty-brown color with an absorption spectrum having maxima at 467, 358, and 288 nm (Figure 5, a). The Mg/Fe LDHs with $x = 0.25$ and 0.33 show a broad absorption starting at 650 nm with peaks in the 350–400 nm range (Figure S1). The LDH with the nominal composition $x = 0.2$ has a single sharp absorption at 280 nm and a light-rose-red color (Figure 5, b). It is our belief that the $x = 0.2$ composition is a single-phase LDH compound, whereas the compositions with $x > 0.2$ have impurities in the form of unitary compounds of Fe^{3+}. These impurities are X-ray

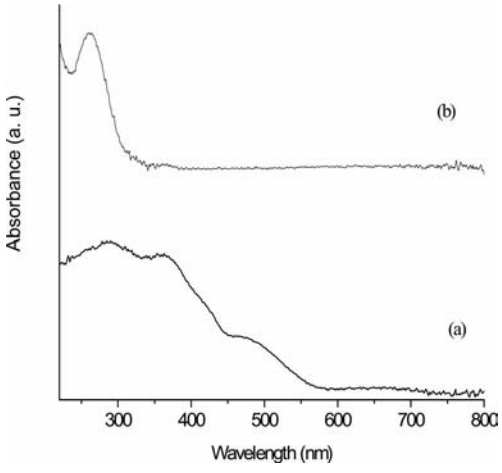

Figure 5. UV/Vis absorption spectra of (a) FeO(OH) and (b) Mg/Fe–CO_3 LDH ($x = 0.2$).

amorphous and are not observed by XRD studies but exhibit signature absorption in the UV/Vis absorption spectra in the region $\lambda > 350$ nm.

Anion-Exchange Reactions of Mg/Fe LDHs

As the carbonate LDHs do not exhibit any exchange reactions, the Mg/Fe–NO_3 LDHs were used for exchange reactions. The NO_3 LDHs were prepared by coprecipitation (pH = 9.5, STAT conditions) with different nominal compositions, x = 0.2–0.33. In all cases, the materials exhibit the expected basal reflections followed by broad peaks with ill-defined maxima in the 2θ = 30–55° region due to the 01l (l = 2,5,8) family of reflections (Figure 6). All the NO_3^- LDHs show the same interlayer spacing of 8 Å. The a parameter estimated from the peak maximum corresponding to the 110 reflection ($a = 2d_{110}$ = 3.01 Å) is also invariant with the nominal composition. This leads us to the conclusion that although all the Mg^{2+} and Fe^{3+} ions are quantitatively precipitated, not all the Fe^{3+} is incorporated within the LDH structure. The actual composition of the LDH phase in all the preparations is constant and is probably close to x = 0.2 ([Mg]/[Fe] = 4). The UV/Vis spectra show (Figure 7) that even among the NO_3^- LDHs, the x = 0.2 composition shows a single sharp absorption at 258 nm, whereas other preparations have absorptions at $\lambda > 350$ nm (Figure S2).

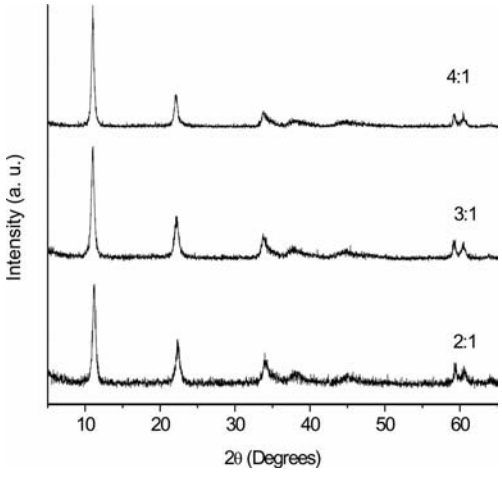

Figure 6. PXRD patterns of Mg/Fe–NO_3 LDHs with different nominal [Mg]/[Fe] ratios.

The NO_3^- LDHs did not exhibit any anion-exchange reactions even over a wide range of pH and temperature. The results of all the exchange reactions are tabulated in Table 5. Substoichiometric uptake of Cl^- and SO_4^- anions was observed, but the LDH after exchange did not show any variation in the interlayer distance, which shows that the uptake is a result of surface adsorption rather than any exchange reaction. The only successful exchange is probably of the nitrate for the carbonate ion from solution.

These observations are understandable on the basis of the following considerations.

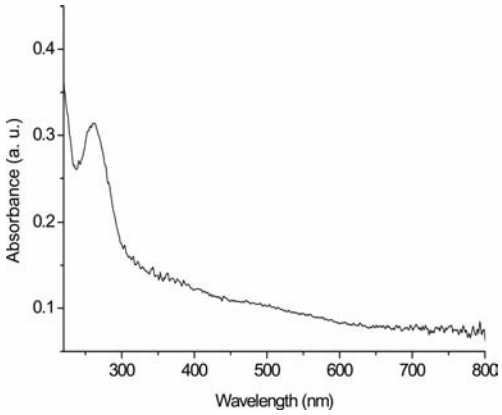

Figure 7. UV/Vis absorption spectrum of the Mg/Fe–NO_3 LDH with a nominal [Mg]/[Fe] ratio of 4.

Table 5. Anion-exchange reactions of the Mg/Fe–NO_3 LDH.

LDH	Anion	Result	LDH	Anion	Result[a]
Mg/Fe–NO_3	CrO_4^{2-}	x	Mg/Fe–NO_3	$Cr_2O_7^{2}$	x
Mg/Fe–NO_3	$[Fe(CN)_6]^{3-}$	x	Mg/Fe–NO_3	SO_4^{2-}	x
Mg/Fe–NO_3	CO_3^{2-}	*	Mg/Fe–NO_3	Cl^-	‡
Mg/Fe–NO_3	ClO_4^-	x	Mg/Fe–NO_3	SCN^-	x
Mg/Fe–NO_3	$[C_2H_4O_6]^{2-}$	x			

[a] x denotes no reaction, ‡ substoichiometric (<0.6 meq g^{-1} of LDH, theoretical capacity is 2.75 meq g^{-1}), and * stands for stoichiometric.

(1) Fe^{3+} has a poor octahedral CFSE, which limits the proportion of Fe^{3+} that can be incorporated into $Mg(OH)_2$. Thus, although other trivalent cations form LDHs over a wide compositional range, $0.2 \leq x \leq 0.33$, Fe^{3+} LDHs are limited to x = 0.2. There is indeed evidence for spinel formation at $T \approx 95$ °C when the Fe^{3+} content is enhanced beyond this limiting value.[38]

(2) Earlier theoretical and experimental work[39,40] has shown that at low values of x (≤0.25) the NO_3^- ion is intercalated in the D_{3h} coordination symmetry with the molecular plane of the nitrate perpendicular to the c crystallographic axis of the LDH. This mode of coordination is similar to that of the CO_3^{2-} ion and greatly stabilizes the intercalated NO_3^- by hydrogen bonding. The NO_3^- ion intercalated in this mode of coordination is nonlabile[39] and does not exchange for other ions from solution.

Conclusions

The Mg/Fe LDH obtained by cation exchange using $Mg(OH)_2$ as a precursor is highly ordered and crystallizes in the $3R_1$ polytype structure (space group $R\bar{3}m$). In this system, the Fe^{3+} content is limited to a value of x = 0.2 and the excess Fe^{3+} precipitates as a binary phase. Consequently these LDHs do not exhibit any anion-exchange properties.

Experimental Section

General: All the reagents, $Mg(NO_3)_2{\cdot}6H_2O$, $Fe(NO_3)_3{\cdot}9H_2O$, Na_2CO_3, $(NH_4)_2CO_3$, NaOH, and aqueous ammonia, were pur-

chased from Merck (India) and used without further purification. Deionized water (specific resistance 15 MΩcm, Millipore Elix-3 water purification system) was used in all the experiments. Three LDH samples were prepared with nominal x values 0.33, 0.25, and 0.20 (these samples are labeled as S1, S2, and S3 respectively). The required amount of Mg^{2+} was precipitated as $Mg(OH)_2$ using 0.5 M $Mg(NO_3)_2$ (S1: 15.2 mL; S2: 17.6 mL; S3: 19.2 mL) and 1 M aqueous ammonia (ca. 25 mL in each case). The precipitated $Mg(OH)_2$ was filtered, washed (with ca. 200 mL of deionized water), and transferred to a 250 mL screw-capped glass bottle and suspended in 150 mL of deionized water. Approximately 20 times the stoichiometric requirement of CO_3^{2-} was added as Na_2CO_3 (S1: 4 g; S2: 3.1 g; S3: 1.3 g) to this slurry. Then the stoichiometric requirement of Fe^{3+} was added in the form of a standard $Fe(NO_3)_3$ solution (1.554 M; S1: 2.4 mL; S2: 1.9 mL; S3: 1.5 mL). In this manner, the Fe^{3+} content was varied to obtain compositions in the range $0.2 \leq x \leq 0.33$. The resultant reaction mixture was stirred for 5 d and the product was divided into two parts. One part was subjected to hydrothermal treatment at 150 °C for 24 h and the other part was filtered, washed, and dried at 65 °C for 24 h.

All the samples were characterized by powder X-ray diffraction (XRD) using a Bruker D8 Advance powder diffractometer (Cu-K_α source, λ = 1.5418 Å) fitted with a secondary monochromator operating in reflection geometry. Data were collected at a continuous scan rate of 1°min^{-1} in steps of 2θ = 0.02°. For Rietveld refinement, data were collected in the 2θ = 5–100° range in steps of 2θ = 0.02° with a counting time of 10 s per step.

The structure refinement of the Mg/Fe–CO_3 LDHs was carried out by using the Rietveld technique with the GSAS[41] software package. For the refinement, a TCH-pseudo-Voigt line shape function (profile function 2) with eight variables was used to fit the experimental profile. The background was corrected by using a 12-coefficient Chebyschev polynomial. Anisotropy in the experimental profile was modeled by using DIFFaX[36] (version 1.807). The interlayer carbonate ion was characterized by FTIR spectroscopy (reflection mode; Bruker Alpha-P; Diamond ATR; 400–4000 cm^{-1}, 4 cm^{-1} resolution). The pH of the reaction medium was monitored by using a digital pH meter (Control dynamics, pH meter APX 175, India). The UV/Vis spectra were recorded with a Shimadzu Model UV-3101 PC UV/Vis/NIR scanning spectrometer fitted with an integrating sphere attachment, Model ISR-3100, for spectral measurement in the diffuse reflectance mode. The powder samples were ground with $BaSO_4$ (Lancaster, England) used as diluents and as well as standard. The thermal behavior of all the samples was studied by TGA (Mettler Toledo TG/SDTA model 851^e system; 30–800 °C; heating rate 5 °C min^{-1}; flow of air). The Mg^{2+} and Fe^{3+} contents of all the LDHs were determined by atomic absorption spectroscopy (Shimadzu AA-6650 spectrometer). The carbonate content was assumed to be half that of Fe^{3+} (x/2). The total intercalated oxygen is expected to be 1 in the empirical formula of the LDH. Therefore the intercalated water was taken to be (1–3x/2); 3x/2 being the contribution of the intercalated carbonate to the oxygen content of the interlayer. In this manner, the approximate formulae of the LDHs were determined. The mass loss due to dehydration obtained from TG data was compared with that expected from the approximate formula (see Table 1).

Further details on the crystal structure investigation may be obtained from the Fachinformationszentrum Karlsruhe, 76344 Eggenstein-Leopoldshafen, Germany (fax: +49-7247-808-666; e-mail: crysdata@fiz-karlsruhe.de), on quoting the depository number CSD-422424.

Supporting Information (see footnote on the first page of this article): Observed and calculated d spacings of the Mg/Fe–CO_3 LDH (x = 0.2), UV/Vis absorption spectra of the Mg/Fe–CO_3 LDHs, and UV/Vis absorption spectra of the Mg/Fe–NO_3 LDHs.

Acknowledgments

The authors thank the Department of Science and Technology (DST) of the Government of India (GOI) for financial support. S. V. P. is a recipient of the Senior Research Fellowship of the Council for Scientific and Industrial Research, GOI. P. V. K. is a recipient of the Ramanna Fellowship of the DST.

[1] a) P. S. Kumbhar, J. Sanchez-Valent, J. M. M. Millet, F. J. Figueras, *J. Catal.* **2000**, *191*, 467; b) P. S. Kumbhar, J. Sanchez-Valent, F. J. Figueras, *Tetrahedron Lett.* **1998**, *39*, 2573; c) R. S. Mulukutla, C. J. Detellier, *J. Mater. Sci. Lett.* **1996**, *15*, 797.
[2] R. Chitrakar, S. Tezuka, A. Sonoda, K. Sakene, T. Hirotsu, *Ind. Eng. Chem. Res.* **2008**, *47*, 4905.
[3] G. Carja, S. Ratoi, G. Ciobanu, I. Balasanian, *Desalination* **2008**, *223*, 243.
[4] S. Aisawa, N. Higashiyama, S. Takahashi, H. Hirahara, D. Ikematsu, H. Kondo, H. Nakayama, E. Narita, *Appl. Clay Sci.* **2007**, *35*, 146.
[5] W. Meng, F. Li, D. G. Evans, X. Duan, *Mater. Res. Bull.* **2004**, *39*, 1185.
[6] M. S. Gasser, H. F. Aly, *Colloids Surf. A* **2009**, *336*, 167.
[7] a) M. Tu, J. Shen, Y. Chen, *J. Solid State Chem.* **1997**, *128*, 73; b) J. Shen, B. Guang, M. Tu, Y. Chen, *Catal. Today* **1996**, *30*, 77.
[8] a) W. Meng, F. Li, D. G. Evans, X. Duan, *Mater. Chem. Phys.* **2004**, *86*, 1; b) F. Li, J. Liu, D. G. Evans, X. Duan, *Chem. Mater.* **2004**, *16*, 1597; c) J. Liu, F. Li, D. G. Evans, X. Duan, *Chem. Commun.* **2003**, 542.
[9] F. Li, Q. Yang, D. G. Evans, X. Duan, *J. Mater. Sci.* **2005**, *40*, 1917.
[10] M. Del Arco, A. Fernandez, C. Martin, V. Rives, *Appl. Clay Sci.* **2009**, *42*, 538
[11] R. Allmann, *Acta Crystallogr., Sect. B* **1968**, *24*, 972.
[12] F. Cavani, F. Trifiro, A. Vaccari, *Catal. Today* **1991**, *11*, 173.
[13] S. Miyata, *Clays Clay Miner.* **1975**, *23*, 369.
[14] A. I. Khan, D. O'Hare, *J. Mater. Chem.* **2002**, *12*, 3191.
[15] I. Pausch, H. H. Lohse, K. Schürmann, R. Allmann, *Clays Clay Miner.* **1986**, *34*, 507.
[16] H. C. B. Hansen, C. B. Koch, *Appl. Clay Sci.* **1995**, *10*, 5.
[17] M. Vucelic, W. Jones, G. D. Moggridge, *Clays Clay Miner.* **1997**, *6*, 803.
[18] R. S. W. Braithwaite, P. J. Dunn, R. G. Pritchard, W. H. Paar, *Min. Mag.* **1994**, *58*, 79.
[19] F. Kovanda, V. Balek, V. Dornicak, P. Martinec, M. Maslan, L. Bilkova, D. Kolousek, I. M. Bountsewa, *J. Therm. Anal. Calorim.* **2003**, *71*, 727.
[20] A. Nakahira, H. Murase, H. Yasuda, *J. Appl. Phys.* **2007**, *101*, 09N516.
[21] D. Dobos, *Electrochemical Data a Handbook for Electrochemist's in Industry and Universities*, Elsevier, Amsterdam, **1975**.
[22] U. Costantino, F. Mormottini, M. Nocchetti, R. Vivani, *Eur. J. Inorg. Chem.* **1998**, *10*, 1439.
[23] N. Iyi, T. Matsumato, Y. Kaneko, K. Kitamura, *Chem. Lett.* **2004**, *33*, 1122.
[24] Y. Han, Z. H. Liu, Z. Yang, Z. Wang, X. Tang, T. Wang, L. Fan, K. Ooi, *Chem. Mater.* **2008**, *20*, 360.
[25] H. R. Oswald, R. Asper, *Bivalent Metal Hydroxides*, in: *Preparation and Crystal Growth of Material With Layered Structure*, vol. I (Ed.: R. M. A. Leith), D. Reidel Publishing Company, Dordrecht, The Netherlands, **1977**, p. 71.
[26] R. D. Shannon, *Acta Crystallogr., Sect. A* **1976**, *32*, 751.
[27] R. K. Allada, A. Navrotsky, H. T. Berbeco, W. H. Casey, *Science* **2002**, *296*, 721.
[28] S. Komarneni, N. Kozai, R. Roy, *J. Mater. Chem.* **1998**, *8*, 1329.

[29] M. C. Richardson, P. S. Braterman, *J. Mater. Chem.* **2009**, *19*, 7965.
[30] G. S. Thomas, P. V. Kamath, *Solid State Sci.* **2006**, *8*, 1181.
[31] J. W. Boclair, P. S. Bratermann, J. Jiang, S. Lou, F. Yarberry, *Chem. Mater.* **1999**, *11*, 303.
[32] W. Kraus, G. Nolze, *POWDERCELL*, v. 2.4, Federal Institute for Materials Research and Training, Berlin, **2000**.
[33] R. Allmann, *Acta Crystallogr., Sect. B* **1968**, *24*, 972.
[34] A. S. Bookin, V. A. Drits, *Clays Clay Miner.* **1993**, *41*, 551.
[35] A. V. Radha, C. Shivakumara, P. V. Kamath, *Clays Clay Miner.* **2005**, *53*, 521.
[36] M. M. J. Treacy, J. M. Newsam, M. W. Deem, *Proc. R. Soc. London A* **1991**, *433*, 499; M. M. J. Treacy, M. W. Deem, J. M. Newsman, *Computer code DIFFaX*, v. 1.807, **2000** (http://www.public.asu.edu/~mtreacy/DIFFaX.html).
[37] R. M. Cornell, U. Schwertmann, *The Iron Oxides: structure, properties, reactions, occurrences and uses*, 2nd ed, Wiley-VCH, Weinheim, Germany, **2003**.
[38] Q. Xu, Y. Wei, Y. Liu, X. Ji, L. Yang, M. Gu, *Solid State Sci.* **2009**, *11*, 472.
[39] H. Li, J. Ma, D. G. Evans, T. Zhou, F. Li, X. Duan, *Chem. Mater.* **2006**, *18*, 4405.
[40] S. L. Wang, P. C. Wang, *Colloids Surf. A* **2007**, *292*, 131.
[41] A. C. Larson, R. B. Von Dreele, *General Structure Analysis System (GSAS)*, Los Alamos National Laboratory Report LAUR 86–748, Los Alamos National Laboratory, Los Alamos, NM, **2004**.

Received: January 30, 2011
Published Online: April 28, 2011

